doi: 10.15407/ujpe61.07.0588

I.O. LYSENKO

Institute of Applied Physics, Nat. Acad. of Sci. of Ukraine
(58, Petropavlivs'ka Str., Sumy 40030, Ukraine; e-mail: lysenko.i@ipfcentr.sumy.ua)

ANALYSIS OF THE FORMATION OF STATIONARY PATTERNS AT THE ION SPUTTERING WITHIN THE ANISOTROPIC KURAMOTO–SIVASHINSKY MODEL

PACS 05.40.Ca, 68.35.Ct, 68.55.J-, 68.55.jm, 79.20.Rf, 81.16.Rf

The processes of change of a surface morphology and formation of a stationary pattern at the ion sputtering are considered. A linear stability analysis was carried out, and the range of parameters, at which the patterning is possible, is determined. Assuming the existence of a stabilization parameter that involves the redistribution of knocked-out atoms, all evolution scenarios for the surface are obtained numerically. The dynamics of defects is numerically analyzed for every structure type, and the corresponding time dependences are plotted.

Keywords: ion sputtering, pattern formation, stationary patterns, heavy ions, ion flux, defect, hexagonal structures, linear structures.

1. Introduction

The study of modifications of the surface morphology in a material sputtered by high-energy particles is a challenging task for modern statistical physics and materials science. Sputtering is one of the most widespread methods applied to the fabrication of thin films and semiconductors and the etching of specimens at the manufacture of integrated circuits and packing devices. It is widely used in micro- and nanoelectronics. It was shown experimentally and theoretically that, under certain conditions, nanostructures can emerge on the surface in the course of sputtering [1–10]. Numerous experimental researches made it possible to establish the key parameters that govern the behavior of a specimen at the sputtering. These are the ion beam flux, energy of incident ions, sputtering angle, and temperature. The experimental researches of the self-organization processes on the surfaces of metals and semiconductors showed that, depending on the energy of an incident particle flux, some stationary patterns can emerge at sputtering. At ion energies of 10^2–10^5 eV, these are the waves or ripples characterized by a certain orientation. Whereas, at ion energies below 10^2 eV, these are isotropic patterns of the nanodot or nanohole type [11–17]. The height of obtained surface patterns changes from 0.1 to 1 μm. The characteristic dimensions of wave patterns vary from 3.5 to 25 nm, and those of nanoholes from 35 to 250 Å [17].

The main theoretical approaches to the study of modifications in the surface morphology are based on the Kardar–Parisi–Zhang model [18]. It was developed by Wolf and Villain [19] and generalized by Kuramoto and Sivashinsky [20]. The described model was applied for the first time by Bradley and Harper, while studying the growth of surface structures at the sputtering [3]. More detailed researches were performed by Cuerno, Barabasi, and Makeev [4, 5]. It was shown that the processes of pattern formation in such systems can be satisfactorily described by the Kuramoto–Sivashinsky equation for the height field on the irradiated surface. The introduction of fluctuations for the surface height field in the form of an ad-

© I.O. LYSENKO, 2016

ditive Langevin source with the intensity proportional to the particle flux allows the statistical origin of surface effects to be studied and the main driving processes of morphological instabilities to be determined for various evolution stages. In the general case, the noise source can also be multiplicative and responsible, e.g., for the sputtering angle spread [21]. In the simplest case, the generalized Bradley–Harper model predicts the formation of only three types of surface patterns. However, if the nonlinearity and anisotropy are taken into account, the spectrum of possible pattern types becomes wider [22].

It is worth noting that the standard solution of the Kuramoto–Sivashinsky equation, which describes the surface profile in the irradiated system and the corresponding patterns, does not predict the formation of a plane surface and the formation of stable patterns that do not change in time. However, this opportunity can be obtained by introducing a component that governs the surface relaxation [23, 24]. In the case of sputtering, this component makes allowance for a possible redistribution of some knocked out atoms over the surface. The evolution of this system in the isotropic case was considered earlier in [25].

The issue concerning the study of possible types of stationary patterns and their properties in case where the dynamics of surface heights at the sputtering is described by the nonlinear anisotropic Kuramoto–Sivashinsky equation with an additive noise, which simulates the fluctuations of the surface height field, remains open. The corresponding anisotropy is a result of the different values of surface tension coefficient. Below, we will analyze the dynamics, types, and conditions of formation of stationary patterns on the surface, as well as the specific features in the influence of the surface dissipation on the created patterns. In addition, we will study the evolution of surface defects.

The work consists of six sections. In Section 2, a model of the system used for the study of variations in the surface morphology taking relaxation processes into account is described. In Section 3, the linear analysis of the stability is carried out. In addition, the phase diagrams, which determine the regions, where the plane and structured surfaces are realized, and the conditions for the stationary pattern formation are obtained. The results of numerical simulation and the diagrams of parameters of the system for various types of structures are presented in Section 4. The evolution of structural defects is analyzed in Section 5. Section 6 contains conclusions.

2. Model

Let us consider a two-dimensional substrate, every point of which at the time moment t is given by the height field $h(\mathbf{r}, t)$, where the vector $\mathbf{r}$ determines the coordinates of a point on the surface. Let us assume that this surface is sputtered by heavy ions of inert gases. In this case, there occurs a series of collisions, so that some atoms are knocked out from their positions and quit the material. As a result, the surface morphology changes, which can result in the formation of patterns. Below, we assume that the surface is located in the plane $x - y$, and the ion flux propagates in the plane $x - z$, with the incidence angle $\theta \in [0, \pi/2]$ reckoned from the normal to the uneroded surface. Then, as was shown in work [26], the energy obtained by the surface in the bulk at its bombardment at a certain point characterized by the coordinates $r(x, y)$ is described by the Gaussian distribution:

$$E(\mathbf{r}) = (\epsilon/(2\pi)^{3/2}\sigma\mu^2)\exp(-z^2/2\sigma^2 - (x^2+y^2)/2\mu^2), \tag{1}$$

where ϵ is the kinetic energy of an incident ion, and σ and μ are the distribution widths in parallel and perpendicularly, respectively, to the sputtering flux.

Expression (1) determines the energy of one incident ion. Actually, the surface is bombarded by a uniform flux J of ions that simultaneously reach the surface. Therefore, the rate of surface erosion depends on the total energy of an incident flux, being determined by the expression

$$v = p \int\limits_{\mathcal{R}} \mathrm{d}\mathbf{r}\Phi(\mathbf{r})E(\mathbf{r}), \tag{2}$$

with the summation carried out over the energy distributions for all ions. In expression (2), $\Phi(x, y, h)$ describes the corrections for local surface slopes in the case of a uniform flux J and looks like $\Phi(x, y, h) = J\cos\left(\arctan\left[\sqrt{(\nabla_x h)^2 + (\nabla_y h)^2}\right]\right)$, and p is a proportionality coefficient depending on the target material properties [26, 27]. Hence, the dynamic equation for the height field $h(x, y, t)$ looks like $\partial_t h \simeq -v(\theta)\sqrt{1 + (\nabla h)^2}$, where $0 < \theta < \pi/2$. In the linear approximation, we obtain

$$\partial_t h = -v_0 + \gamma\nabla_x h + \nu_x\nabla^2_{xx}h + \nu_y\nabla^2_{yy}h, \tag{3}$$

where the quantity v_0 is the rate constant for surface erosion, $\gamma = \gamma(\theta)$ describes the dependence of the erosion on the inclination angle of a bombarding ion flux, and $\nu_{x,y} = \nu_{x,y}(\theta)$ are the effective coefficients of surface tension induced by the erosion processes along each direction. The anisotropy of the obtained system is determined by different values of erosion propagation coefficients ν_x and ν_y along the directions x and y, respectively.

Equation (3) has to be generalized by introducing the surface flux into consideration. This parameter is given by the expression $j_s = K\nabla(\nabla^2 h)$, where $K > 0$ is the temperature-dependent constant of the surface diffusion. The account for the first nonlinear terms in the series expansion of the rate v in the height gradient allows the dynamic equation for the height field $h' = h + v_0 t$ [3, 4] to be obtained in the form

$$\frac{\partial h}{\partial t} = \gamma\frac{\partial h}{\partial x} + \nu_x\frac{\partial^2 h}{\partial x^2} + \nu_y\frac{\partial^2 h}{\partial y^2} + \\ + \frac{\lambda_x}{2}\left(\frac{\partial h}{\partial x}\right)^2 + \frac{\lambda_y}{2}\left(\frac{\partial h}{\partial y}\right)^2 - K\nabla^4 h + \xi(x,y,t), \qquad (4)$$

where, for convenience, the prime sign is omitted, and the additive noise ξ is introduced. We suppose that the Langevin noise source in Eq. (4) has the Gaussian-like properties, i.e.

$$\langle\xi(\mathbf{r},t)\rangle = 0, \\ \langle\xi(\mathbf{r},t)\xi(\mathbf{r}',t)\rangle = 2\Sigma\delta(\mathbf{r}-\mathbf{r}')\delta(t-t'), \qquad (5)$$

where Σ determines the intensity of surface height fluctuations. As was shown in work [5], the coefficients in Eq. (4) look like

$$\gamma = F_0\frac{s}{f^2}\left(a_\sigma^2 a_\mu^2 c^2(a_\sigma^2 - 1) - a_\sigma^4 s^2\right), \qquad (6)$$

$$\nu_x = F_0\frac{a_\sigma^2}{2f^3}\left(2a_\sigma^4 s^4 - a_\sigma^4 a_\mu^2 s^2 c^2 + a_\sigma^2 a_\mu^2 s^2 c^2 - a_\mu^4 c^4\right), \qquad (7)$$

$$\nu_y = -F_0\frac{c^2 a_\sigma^2}{2f}, \qquad (8)$$

$$\lambda_x = F_0\frac{c}{2f^4}\Big(a_\sigma^8 a_\mu^2 s^4(3+2c^2) + \\ + 4a_\sigma^6 a_\mu^4 c^4 s^2 - a_\sigma^4 a_\mu^6 c^4(1+2s^2) - \\ - f^2(2a_\sigma^4 s^2 - a_\sigma^2 a_\mu^2(1+2s^2)) - a_\sigma^8 a_\mu^4 s^2 c^2 - f^4\Big), \qquad (9)$$

$$\lambda_y = -F_0\frac{c}{2f^2}\left(a_\sigma^4 s^2 + a_\sigma^2 a_\mu^2 c^2 - a_\sigma^4 a_\mu^2 c^2 - f^2\right). \qquad (10)$$

In expressions (6)–(10), the quantity F_0 is defined as follows:

$$F_0 \equiv \frac{J\varepsilon p a}{\sigma\mu\sqrt{2\pi f}}\exp\left(\frac{-a_\sigma^2 a_\mu^2 c^2}{2f}\right).$$

The other quantities are $a_\sigma \equiv \frac{a}{\sigma}$, $a_\mu \equiv \frac{a}{\mu}$, $s = \sin\theta$, $c = \cos\theta$, and $f = a_\sigma^2 s^2 + a_\mu^2 c^2$.

The Kuramoto–Sivashinsky equation written in the form (4) has no solutions that would characterize a plane surface and describe the formation of stationary patterns. As a rule, the surface height and the pattern arrangement permanently and chaotically change, although the dimensions and the number of patterns remain constant [28]. However, the stationary state can be reached by introducing a linear term $-\alpha h$ into the equation, which will govern the processes of height relaxation on the irradiated surface owing to the redistribution of atoms knocked out from it [29]. Hence, the stationary anisotropic Kuramoto–Sivashinsky equation reads

$$\frac{\partial h}{\partial t} = -\alpha h + \gamma\frac{\partial h}{\partial x} + \nu_x\frac{\partial^2 h}{\partial x^2} + \nu_y\frac{\partial^2 h}{\partial y^2} + \\ + \frac{\lambda_x}{2}\left(\frac{\partial h}{\partial x}\right)^2 + \frac{\lambda_y}{2}\left(\frac{\partial h}{\partial y}\right)^2 - K\nabla^4 h + \xi(x,y,t). \qquad (11)$$

All parameters are determined by the target material and irradiation conditions, namely, the ion penetration depth a, angle of sputtering flux incidence θ, flux J, and kinetic energy of ions ε.

3. Linear Analysis of Stability

Let us perform a linear analysis of stability to determine the ranges of parameters, in which either the plane surface is formed or the pattern formation takes place. For this purpose, we should average Eq. (11) over the noise. As a result, we obtain an equation for the first statistical moment in the form

$$\frac{\partial}{\partial t}\langle h\rangle = -\alpha\langle h\rangle + \gamma\frac{\partial}{\partial x}\langle h\rangle + \nu_x\frac{\partial^2}{\partial x^2}\langle h\rangle + \nu_y\frac{\partial^2}{\partial y^2}\langle h\rangle + \\ + \frac{\lambda_x}{2}\left\langle\left(\frac{\partial h}{\partial x}\right)^2\right\rangle + \frac{\lambda_y}{2}\left\langle\left(\frac{\partial h}{\partial y}\right)^2\right\rangle - K\nabla^4\langle h\rangle, \qquad (12)$$

where the properties of noise (5) are taken into account.

Let us consider the stability of a linearized system. In this case, all nonlinear terms are neglected, and we obtain

$$\frac{\partial}{\partial t}\langle h\rangle = -\alpha\langle h\rangle + \gamma\frac{\partial}{\partial x}\langle h\rangle + \nu_x\frac{\partial^2}{\partial x^2}\langle h\rangle + \\ + \nu_y\frac{\partial^2}{\partial y^2}\langle h\rangle - K\nabla^4\langle h\rangle. \quad (13)$$

In the deterministic case or in the presence of an additive white noise, the linearized equation is known to allow a solution in the form

$$\langle h(x,y,t)\rangle = A\exp[i(k_x x + k_y y - \omega t) + rt].$$

Substituting it into Eq. (13), we find the following expressions for the frequency ω and the stability parameter r:

$$\omega = -\gamma(\theta)k_x, \\ r = -\alpha - \nu_x k_x^2 - \nu_y k_y^2 - K(k_x^2 + k_y^2)^2. \quad (14)$$

As was shown in work [29], the stabilization parameter α has a certain critical value α_c, at which stationary patterns can be formed in the system concerned. Hence, the surface becomes plane at $\alpha > \alpha_c$; otherwise, the spatial patterns become unstable. The analysis of the corresponding dependences $\alpha(k_x, k_y, k_z)$ demonstrates that the number of unstable modes substantially decreases, when α tends to its critical value α_c. The realization of a plane surface evidently corresponds to etching processes. In the general case, the quantity α_c depends on the energy of incident ions, incidence angle, and temperature of the irradiated surface.

The corresponding dependences of α_c on the main parameters of the system are depicted in Fig. 1. The parameter regions, in which the formation of spatially modulated patterns is possible, are located below the plotted surfaces. In the regions above the surfaces, we obtain a plane homogeneous surface. From Fig. 1, *a*, one can see that, provided the ratio between the penetration depth and the transverse width of the spread is fixed, the behavior of the critical value α_c on the sputtering angle is not monotonic, so that α_c has a maximum. From the monotonically decreasing dependence $\alpha_c(\theta, a_\mu)$ exhibited in Fig. 1, *b*, it follows that, when the incidence angle and the quantity a_μ grow at a fixed spread width σ, the stationary patterns are realized at small α_c-values.

4. Numerical Simulation

Let us consider the behavior of the anisotropic nonlinear model (11) in the cases $\lambda_x \neq 0$ and $\lambda_y \neq 0$ by setting $\gamma = 0$.

The change of signs of the parameters ν_x, ν_y, and λ_x is known to result in a variation of the created surface patterns. The parameter ν_y is always negative ($\nu_y < 0$), as is seen from expression (10), whereas the other parameters can change their sign. The corresponding phase diagrams are depicted in Fig. 2. Let us consider the diagram exhibited in Fig. 2, *a*, which

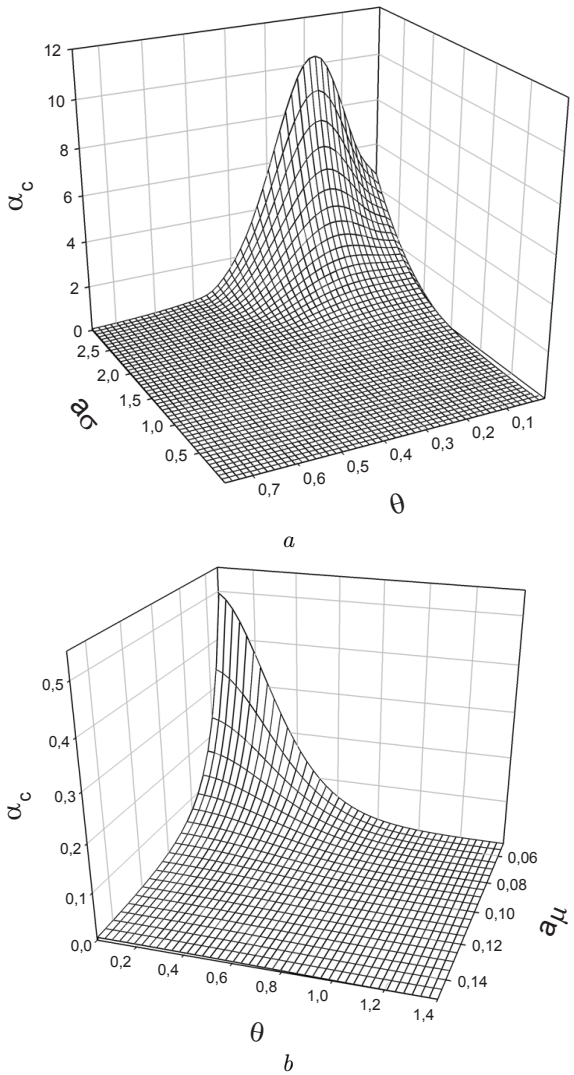

Fig. 1. Phase diagrams for the linear analysis of the stability of the system at $a_\mu = 1.0$ (*a*) and 0.1 (*b*). For all panels, $F_0 = 1$, $K = 2$

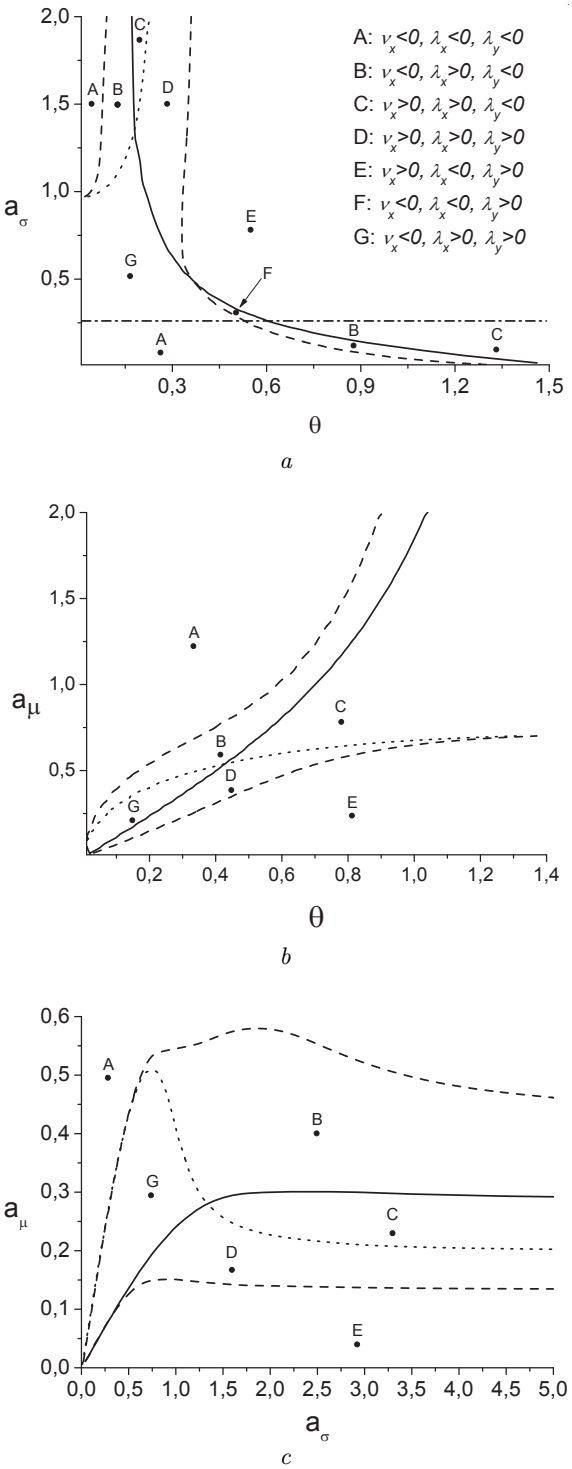

a *b* *c*

Fig. 2. Phase diagrams for the nonlinear anisotropic system at $a_\mu = 0.25$ (*a*), $a_\sigma = 1.0$ (*b*), and $\theta = 0.2$ (*c*). For all panels, $F_0 = 1$, $K = 2$, and $\Sigma = 1$

was plotted for $a_\mu = 0.25$. One can see that the (a_σ, θ)-plane is divided into seven regions, in which patterns with different morphologies are realized. The solid curve marks the change of the ν_x-sign, the dashed one corresponds to the change of the λ_x-sign, and the dotted one was calculated at $\lambda_y = 0$. The dash-dotted curve that separates the regions at the diagram bottom was determined from the condition of the simultaneous change of the λ_x- and λ_y-signs. According to the diagram shown in Fig. 2, *b* plotted at $a_\sigma = 1.0$, one can observe the variation of the existence domains for the patterns of various types. The dependences of the dimensionless lengths at a fixed sputtering angle, which determine the change of the corresponding pattern types and the domains of their existence, can be seen in Fig. 2, *c*. It is worth noting that if $a_\sigma \leq a_\mu$, only the first three regions–A, B, and C–are realized [21, 25].

Let us analyze the surface dynamics in the obtained regions of the phase diagrams shown in Fig. 2. Using a numerical simulation, we intend to solve Eq. (11) on a discrete $N \times N$ lattice, where $N = 256$, with periodic boundary conditions. The lattice period $\ell = 1$, and the step of integration over the time $\Delta t = 0.005$.

4.1. Behavior of the System in Regions A, B, and C

Let us analyze the behavior of the system in regions A, B, and C, for which $a_\sigma \leq a_\mu$. The surface evolution, when the value of the parameter α is close to the critical point, is shown in Fig. 3. Here, the dark regions correspond to smaller height field values, and the light regions to larger ones. One can see that the stationary patterns are developed in time in the region A ($\nu_x < 0$, $\lambda_x < 0$, and $\lambda_y < 0$). They look like holes confined by walls and have the hexagonal symmetry slightly violated by point defects. The region of parameters B ($\nu_x < 0$, $\lambda_x > 0$, and $\lambda_y < 0$) is characterized by the formation of a linear surface pattern with defects. In region C ($\nu_x > 0$, $\lambda_x > 0$, and $\lambda_y < 0$), we obtain similar linear surface patterns, but with a shorter period and the absence of defects. The width of the corresponding interface region (Fig. 4) grows most rapidly for region C and most slowly for region B.

Let us consider the influence of the parameter α, which governs the redistribution of knocked-out atoms, on the behavior of the anisotropic nonlinear

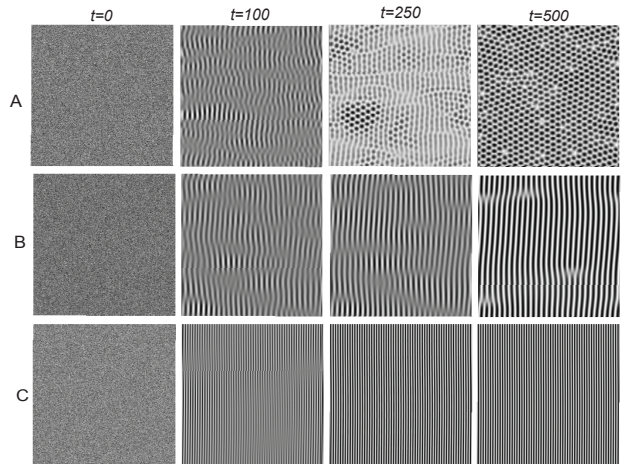

Fig. 3. Evolution of the anisotropic nonlinear system in a vicinity of the critical stabilization parameter α_c in regions A, B, and C. The dimensions of each region equal $N \times N = 256 \times 256$

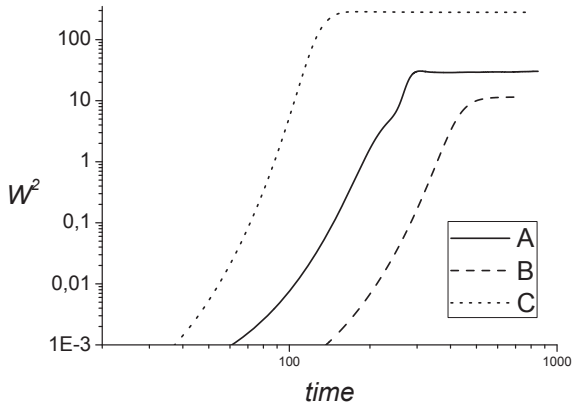

Fig. 4. Dynamics of the interface width for regions of parameters A, B, and C

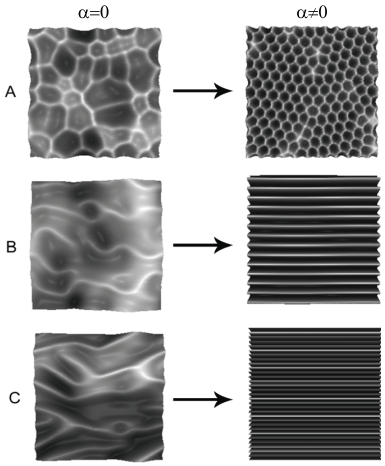

Fig. 5. Comparison of the evolution of the system at $\alpha = 0$ and in a vicinity of the critical point α_c in regions A, B, and C

system in more details. For this purpose, let us compare the surface evolution at $\alpha = 0$ and $\alpha \neq 0$. The created surface patterns for those regions in the absence of the stabilization parameter α were analyzed earlier in works [3–5, 21]. The left panels in Fig. 5 demonstrate the known solution of Eq. (11) obtained at $\alpha = 0$. The obtained patterns are unstable, and the surface height permanently changes. However, the account of surface relaxation processes allows the stationary state to be obtained in a vicinity of the critical point α_c (right panels in Fig. 5).

4.2. Behavior of the System in Regions D, E, F, and G

Now, let us consider the behavior of the nonlinear anisotropic system in regions D, E, F, and G at $\alpha \neq 0$. As one can see from Fig. 6, in a vicinity of the critical point α_c, linear patterns are formed on the surface in all examined regions. The difference consists in the period of created surface patterns and the presence of surface defects. In region D ($\nu_x > 0$, $\lambda_x > 0$, and $\lambda_y > 0$), patterns with the shortest period and the lowest linear defect presence are formed, which persist in time. A similar pattern with defects, but with a longer pattern period is formed in region F ($\nu_x < 0$, $\lambda_x < 0$, and $\lambda_y > 0$). Regions E ($\nu_x > 0$, $\lambda_x < 0$, and $\lambda_y > 0$) and G ($\nu_x < 0$, $\lambda_x > 0$, and $\lambda_y > 0$) are characterized by the total absence of any linear defects on the linearly structured stationary surface; but the pattern period is longer in region E.

5. Research of Defects on the Surface

Let us analyze the evolution of the defect number. For this purpose, let us consider the defect concentration N_{def}/N^2, where N_{def} is the total number of surface defects at every time moment, and N the discrete lattice size (in our case, $N = 256$).

If the patterns formed on the surface have the hexagonal symmetry (region A), the number of surface defects was determined, by using an algorithm developed for the analysis of two-dimensional systems obtained by the molecular dynamics method [30]. In this case, the patterns can be represented as atoms,

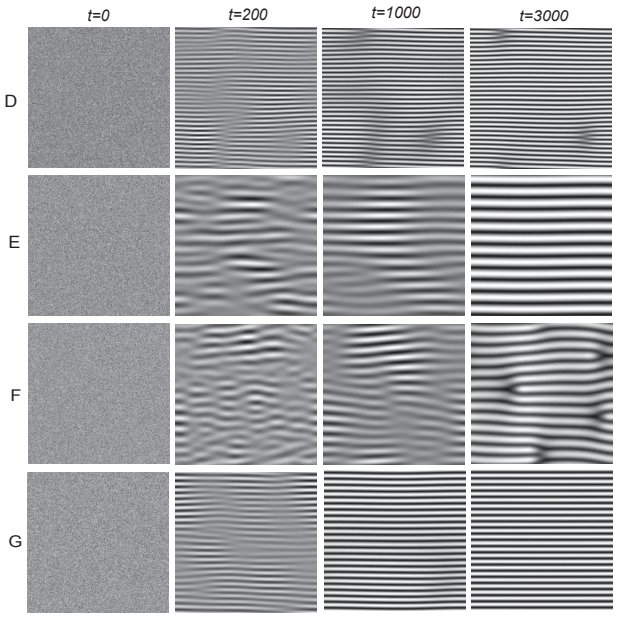

Fig. 6. Evolution of the anisotropic nonlinear system in a vicinity of the critical stabilization parameter α_c in regions D, E, F, and G. The dimensions of each region equal $N \times N = 256 \times 256$

and the local crystalline order is given by the orientation of hexagons, the vertices of which give the pattern positions. As was shown in work [30], the orientation angle of the j-th atom, $\phi_j \in [0, \pi/3]$, can be determined from the formula

$$\Psi_j = \sum_{k \in nn(j)} \exp[6i\theta_{jk}] = |\Psi_j| \exp^{6i\phi_j}.$$

Two atoms are considered to be neighbors, if $|r_j - r_k| < 1.25v$, where v is the position of the first peak in the two-particle correlation function, and θ_j is the angle between the vector $\mathbf{r}_j - \mathbf{r}_k$ and the axis x. To determine the number of defects, analogously to the search for atoms with packing defects, the disorder degrees are calculated for every atom using the formula

$$D_j = 2 \sum_{k \in nn(j)} [1 - \cos 6(\phi_j - \phi_k)].$$

While studying the linear defects, let us apply the approach developed for the search for dislocations and disclinations in nematics [31]. For this purpose, we have to define such order criteria as the director

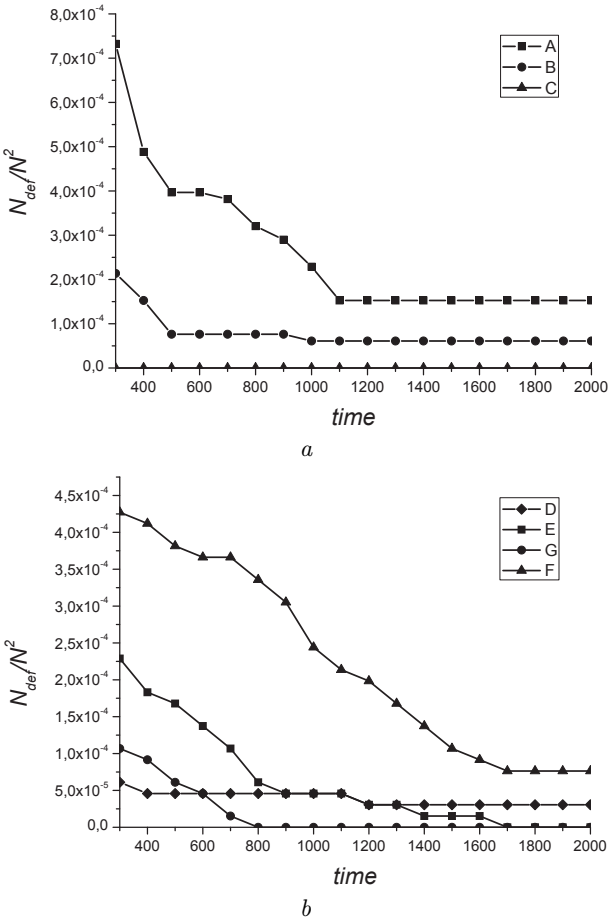

Fig. 7. Evolution of the surface defect concentration at the ion sputtering for regions A, B, and C (a) and D, E, F, and G of parameters (b)

field $\hat{n}(\mathbf{r}) = \frac{\nabla h(\mathbf{r})}{|\nabla h(\mathbf{r})|}$ and the corresponding nematic order parameter $Q_{\alpha\beta} = Q_0 \left[\hat{n}_\alpha \hat{n}_\beta - \frac{1}{2}\delta_{\alpha\beta}\right]$. It is known that, in the case of two-dimensional systems, the role of order parameter is played by the quantity $\cos 2\theta$, where $\hat{n} = (\cos\theta, \sin\theta)$. In other words, there exists a certain vector order parameter $\hat{\mathbf{B}}$ defined by the expressions $\hat{B}_x = \hat{n}_x^2 - \hat{n}_y^2$ and $\hat{B}_y = 2\hat{n}_x\hat{n}_y$. It is known that all defects are formed from $\pm\frac{1}{2}$-disclinations in the field of the director $\hat{n}$, which transforms into the ± 1-charge perturbation for the field $\hat{\mathbf{B}}$. The perturbation is determined by the formula $A = \sum_{\alpha,\beta}(\nabla_\alpha B_\beta)^2$. The expression for A can be written in another form,

$$A = \sum_{\alpha,\beta}(\nabla_\alpha n_\beta)^2 = (\nabla_\alpha \varphi)^2,$$

where $\varphi(\mathbf{r},t) = 2\theta(\mathbf{r},t)$ and $\theta(\mathbf{r}) = \arctan\left(\frac{\hat{n}_y(\mathbf{r})}{\hat{n}_x(\mathbf{r})}\right)$. The nematic order parameter $Q_{\alpha\beta}$ is completely determined by the angle $\varphi(\mathbf{r}) = 2\theta(\mathbf{r})$. Thus, knowing the derivative $\nabla\varphi(\mathbf{r})$, we can determine the quantity $A(\mathbf{r}) = |\nabla\varphi(\mathbf{r})|^2$. Near a defect, the value of $\hat{\mathbf{B}}$ drastically changes. Therefore, in the region far from defects, we have $A(\mathbf{r}) \approx 0$. The value of $A(r)$ drastically grows near a defect location place. So, if the quantity $A(r)$ becomes rather large at a certain point $\mathbf{r}$, this is a point where a defect is located.

The described algorithm helps us to detect the regions where the director field considerably changes and register the corresponding points. However, those points still have to be grouped into patterns. The elements of the same pattern are located very close to one another, but not obligatorily in neighbor cells. Therefore, it is expedient to introduce a filter parameter a_0, which gives a distance between the points. If the distance between the points is shorter than a_0, they are considered to belong to the same pattern. To distinguish between such point clusters, the Hoshen–Kopelman method was used [32].

The obtained time dependences for the defect concentration in various A to F regions are shown in Fig. 7. One can see that, in regions A, B, D, and F, the defect concentration decreases in time, but the defect number does not vanish. At the same time, in regions E and G, the defect concentration falls down to zero, when the surface reaches the stationary regime. In region C, the defect concentration does not decrease in time, because it always equals zero. It is worth noting that defects of only one characteristic type, dislocations, were identified for linear patterns, whereas disclinations and grain boundaries were not observed at the ion sputtering.

6. Conclusions

The behavior of a surface subjected to the ion sputtering under conditions where stationary surface patterns are formed has been studied, by using the nonlinear anisotropic Kuramoto–Sivashinsky equation. To reach the stationary regime in the behavior of the irradiated surface, relaxation processes taking place owing to the redistribution of knocked-out atoms are made allowance for. The linear analysis of the stability of this system is carried out, and the corresponding phase diagrams were plotted. They divide the region of main control parameters into sections, in which either the plane surface is realized or surface patterns emerge. The phase diagrams determining the change of pattern morphology on the surface are obtained within the nonlinear model. It is found that at most seven different regions of parameters may exist for the nonlinear anisotropic system.

On the basis of this information and using a numerical simulation, the Kuramoto–Sivashinsky equation is solved on a square discrete lattice with periodic boundary conditions, and the types of stationary patterns are determined for all regions in the phase diagram. It is found that two types of stationary patterns can be formed on the surface: hexagonal and linear ones. The linear surface formations in different regions differ by their dimensions and defect concentration. Using two types of algorithms for each pattern type, the dynamics of defects on the surface is analyzed. It is found that the concentration of defects decreases in time and, under certain conditions, vanishes. It is also found that there exists a region of parameters, in which the defect-free pattern may be formed.

The results of this work can be useful for studying the structuring processes at the ion sputtering of materials and to manufacture devices, in which the structures of a given geometry are used.

1. M. Navez, C. Sella, and D. Chaperot, *Ionic Bombardment: Theory and Applications* (Gordon and Breach, New York, 1964).
2. L. Jacak, P. Hawrylak, and A. Wojs, *Quantum Dots* (Springer, Berlin, 1998).
3. R.M. Bradley and J.M. E. Harper, J. Vac. Sci. Technol. A **6**, 2390 (1988).
4. R. Cuerno and A.-L. Barabasi, Phys. Rev. Lett. **74**, 4746 (1995).
5. M. Makeev and A.-L. Barabasi, Appl. Phys. Lett. **71**, 2800 (1997).
6. J.T. Drotar, Y.-P. Zhao, T.-M. Lu, and G.-C. Wang, Phys. Rev. E **59**, 177 (1999).
7. T. Aste and U. Valbusa, Physica A **332**, 548 (2004).
8. B. Kahng and J. Kim, Curr. Appl. Phys. **4**, 115 (2004).
9. R. Kree, T. Yasseri, and A. K. Hartmann, Nucl. Instrum. Methods B **267**, 1407 (2009).
10. V.O. Kharchenko and D.O. Kharchenko, Condens. Matter Phys. **14**, 23602, (2011).
11. S. Rusponi, C. Boragno, and U. Valbusa, Phys. Rev. Lett. **78**, 2795 (1997).
12. S. Rusponi, G. Costantini, C. Boragno, and U. Valbusa, Phys. Rev. Lett. **81**, 2735 (1998).
13. E. Chason, T.M. Mayer, B.K. Kellerman, D.T. McIlroy, and A.J. Howard, Phys. Rev. Lett. **72**, 3040 (1994).

14. J. Erlebacher, M.J. Aziz, and E. Chason, Phys. Rev. Lett. **82**, 2330 (1999).
15. W.-Q. Li, L.J. Qi, and X. Yang, Appl. Surf. Sci. **252**, 7794 (2006).
16. J. Lian, Q.M. Wei, L.M. Wang, L.M. Wang, and L.A. Boatner, Appl. Phys. Lett. **88**, 093112 (2006).
17. S. Facsko, T. Dekorsy, and C. Koerdt, Science **285**, 1551 (1999).
18. M. Kardar, G. Parisi, and Y.-C. Zhang, Phys. Rev. Lett. **56**, 889 (1986).
19. D.E. Wolf and J. Villian, Europhys. Lett. **13**, 389 (1990).
20. Y. Kuramoto and T. Tsuzuki, Prog. Theor. Phys. **55**, 356 (1976).
21. D.O. Kharchenko, V.O. Kharchenko, I.O. Lysenko, and S.V. Kokhan, Phys. Rev. E **82**, 061108 (2010).
22. V.O. Kharchenko, Funct. Mater. **18**, 156 (2011).
23. C. Misbah and A. Valance, Phys. Rev. B **49**, 166 (1994).
24. M. Paniconi and K.R. Elder, Phys. Rev. E **56**, 2713 (1997).
25. I.O. Lysenko, D.O. Kharchenko, S.V. Kokhan, and A.V. Dvornichenko, Metallofiz. Noveish. Tekhnol. **35**, 763 (2013).
26. P. Sigmund, Phys. Rev. **184**, 383 (1969).
27. M. Makeev, R. Cuerno, and A.-L. Barabasi, NIMB **197**, 185 (2002).
28. V. O. Kharchenko, Funct. Mater. **18**, 156 (2011).
29. I. Bena, C. Misbah, and A. Valance, Phys. Rev. B **47**, 12 (1993).
30. T. Yamanaka and A. Onuki, Phys. Rev. E **77**, 042501 (2008).
31. Hai Qian, G.F. Mazenko, Phys. Rev. E **73**, 036117 (2006).
32. H. Gould and J. Tobochnik, *An Introduction to Computer Simulation Methods, Part 2*, (Addison-Wesley, Reading, MA, 1988).

Received 24.09.15.
Translated from Ukrainian by O.I. Voitenko

І.О. Лисенко

ФОРМУВАННЯ СТІЙКИХ ПОВЕРХНЕВИХ СТРУКТУР ПРИ ІОННОМУ РОЗПОРОШЕННІ В РАМКАХ АНІЗОТРОПНОЇ МОДЕЛІ КУРАМОТО–СІВАШИНСЬКОГО

Р е з ю м е

Розглянуто процеси зміни морфології поверхні з утворенням стаціонарних структур при іонному розпорошенні. Проведено лінійний аналіз на стійкість та визначено області параметрів, у яких можливе структуроутворення. Чисельно отримано всі можливі картини поведінки поверхні за умови наявності параметра стабілізації, що враховує перерозподіл вибитих атомів. Методами числового аналізу виконано аналіз динаміки дефектів для кожного типу поверхневих структур та побудовано відповідні часові залежності.